Periostin promotes renal cyst growth and interstitial fibrosis in polycystic kidney disease

Darren P. Wallace[1,2,5], **Corey White**[1,5], **Lyudmyla Savinkova**[1,5], **Emily Nivens**[1,5], **Gail A. Reif**[1,5], **Cibele S. Pinto**[1,5], **Archana Raman**[2,5], **Stephen C. Parnell**[4,5], **Simon J. Conway**[6], and **Timothy A. Fields**[3,5]

[1]Department of Medicine, University of Kansas Medical Center, Kansas City, Kansas, United States

[2]Department of Molecular and Integrative Physiology, University of Kansas Medical Center, Kansas City, Kansas, United States

[3]Department of Pathology, University of Kansas Medical Center, Kansas City, Kansas, United States

[4]Department of Biochemistry and Cellular Biology, University of Kansas Medical Center, Kansas City, Kansas, United States

[5]The Kidney Institute, University of Kansas Medical Center, Kansas City, Kansas, United States

[6]Herman B Wells Center for Pediatric Research, Indiana University School of Medicine, Indianapolis, Indiana

Abstract

In renal cystic diseases, sustained enlargement of fluid-filled cysts is associated with severe interstitial fibrosis and progressive loss of functioning nephrons. Periostin, a matricellular protein, is highly overexpressed in cyst-lining epithelial cells of autosomal dominant polycystic disease kidneys (ADPKD) compared to normal tubule cells. Periostin accumulates *in situ* within the matrix subjacent to ADPKD cysts, binds to $\alpha_V\beta_3$- and $\alpha_V\beta_5$-integrins and stimulates the integrin-linked kinase to promote cell proliferation. We knocked out periostin (*Postn*) in *pcy/pcy* mice, an orthologous model of nephronophthisis type 3, to determine whether periostin loss reduces PKD progression in a slowly progressive model of renal cystic disease. At 20 weeks of age, *pcy/pcy: Postn−/−* mice had a 34% reduction in kidney weight/body weight, a reduction in cyst number and total cystic area, a 69% reduction in phosphorylated S6, a downstream component of the mTOR pathway, and fewer proliferating cells in the kidneys compared to *pcy/pcy: Postn+/+* mice. The *pcy/pcy Postn* knockout mice also had less interstitial fibrosis with improved renal function at 20 weeks and significantly longer survival (51.4 compared to 38.0 weeks). Thus, periostin adversely modifies the progression of renal cystic disease by promoting cyst epithelial cell

Correspondence to: Darren P. Wallace, Ph.D., The Kidney Institute, Department of Medicine, University of Kansas Medical Center, 3901 Rainbow Boulevard, Kansas City, KS 66160-3018, dwallace@kumc.edu.

proliferation, cyst enlargement and interstitial fibrosis, all contributing to the decline in renal function and premature death.

Keywords

integrins; proliferation; ADPKD; osteoblast specific factor 2; integrin-linked kinase

INTRODUCTION

Polycystic kidney disease (PKD) is a family of hereditary disorders characterized by the formation and progressive expansion of numerous fluid-filled cysts that cause massively enlarged kidneys (1). Renal cysts are benign neoplasms that ultimately cause renal insufficiency through extensive nephron loss and replacement of normal parenchyma with fibrosis (2). Autosomal dominant PKD (ADPKD) is the most common inherited renal disorder with a frequency of 1:500 individuals and accounts for 7–9% of patients on renal replacement therapy. ADPKD is caused by mutations in *PKD1* or *PKD2*, genes that encode polycystin-1 (PC1) and polycystin-2 (PC2), respectively (3–6). Autosomal recessive PKD (ARPKD) is less common (~1:20,000 births) and is caused by mutations in *PKHD1*, a gene that encodes fibrocystin. ARPKD is characterized by rapid disease progression, often leading to renal failure within the first year of life. Several signaling pathways, including those regulated by cAMP, growth factors, B-Raf/MEK/ERK, mammalian Target Of Rapamycin (mTOR), integrins, and Akt have been implicated in aberrant cell proliferation and the relentless expansion of PKD cysts (7–16).

In addition to intrinsic defects in PKD cells, factors secreted into the extracellular environment may also contribute to cyst growth and development of interstitial fibrosis. We and others have shown that mRNA levels of genes involved in tissue remodeling and extracellular matrix (ECM) production are highly elevated in cystic cells compared to normal renal cells (12, 17). In fact, periostin was one of the most highly differentially expressed genes in human ADPKD cells compared to normal tubule cells (12). Periostin is a secreted protein that binds to components of the ECM, including type I collagen and fibronectin, and has been implicated in collagen fibrillogenesis (18–20). Periostin, as well as other "matricellular" proteins, transmits signals from the ECM to the cell by binding to cell surface integrins, leading to changes in cell adhesion, migration, proliferation, survival and tissue angiogenesis (21–26). While periostin is expressed in several tissues during embryonic development (27, 28), its expression in adults is restricted to collagen-rich tissues and can be upregulated by mechanical stress (29–31). Periostin has also been found to be elevated in a variety of cancers, including breast, lung, and colon, where it promotes cell proliferation and survival (21, 22, 25, 32–36).

In ADPKD, periostin is secreted by cyst-lining cells and accumulates within the ECM adjacent to cysts (12). Periostin binds $\alpha_V\beta_3$ and $\alpha_V\beta_5$ integrins and stimulates integrin-linked kinase (ILK), leading to an acceleration of cell proliferation and *in vitro* cyst growth of ADPKD cells within a collagen matrix. By contrast, periostin does not stimulate the proliferation of normal renal cells, suggesting that periostin is a novel autocrine mitogen

secreted by cystic cells (12). In this study, we show that upregulation of periostin expression is not limited to ADPKD, but rather is a common feature of inherited renal cystic epithelia, regardless of the underlying genetic defect. To determine if periostin contributes to PKD progression, we knocked out periostin (*Postn*) expression in *pcy/pcy* mice, a well characterized model orthologous to human nephronophthisis type three, a recessive form of PKD that typically causes renal failure in children and adolescents (37, 38). In *pcy/pcy* mice, cystic kidneys enlarge to several times normal size and are associated with extensive renal interstitial fibrosis by 18 weeks of age and the development of azotemia (37). Previously, we monitored PKD progression in a *pcy/pcy* mouse by measuring kidney volume by magnetic resonance imaging. Kidney volume increased exponentially up to 20 weeks of age, after which there was a plateau as renal parenchyma was replaced with fibrosis (39). In this study, we determined if loss of *Postn* expression reduced kidney weight, cystic index, cell proliferation and fibrosis in 20-week old *pcy/pcy* mice and extended their survival. The results indicate that periostin and its associated signaling pathways may be viable targets for therapy in PKD.

RESULTS

Periostin expression in pcy/pcy kidneys

Periostin (*Postn*) mRNA is highly overexpressed in human ADPKD cyst epithelial cells compared to normal human kidney cells (12). Similarly, we found that *Postn* is overexpressed in ARPKD and several animal models of cystic disease (Table 1), suggesting that aberrant periostin expression is a general feature of PKD, regardless of the underlying genetic mutation.

To determine if periostin was increased in cystic kidneys of *pcy/pcy* mice, we compared *Postn* expression to WT mice at 1, 10 and 20 weeks. Kidney volume of *pcy/pcy* mice was elevated at 1 week and continued to increase to 20 weeks (Fig. 1a), as described previously (39). By contrast, body weight of *pcy/pcy* mice was reduced compared to WT mice (Fig. 1b). At 20 weeks, periostin mRNA (Fig. 1c) and protein (Fig. 1d, Supplemental Figure S1) were elevated in *pcy/pcy* kidneys compared to age-matched WT kidneys, confirming that periostin is overexpressed in this model of slowly progressive renal cystic disease.

Effects of periostin on body and kidney mass and renal cystic disease

Periostin knockout mice have been reported previously (40). Consistent with this report, sex-matched *Postn*$^{-/-}$ mice were similar in general appearance to WT (*Postn*$^{+/+}$) littermates (not shown). Also as reported, 20-week old *Postn*$^{-/-}$ mice exhibited a moderate reduction in body weight compared to WT littermates (36.8 ± 1.1 g for WT *vs.* 31.6 ± 0.9 g for the *Postn*$^{-/-}$, $P < 0.005$) (Fig. 2a). However, there was no difference in total kidney weight (both kidneys) between *Postn*$^{-/-}$ and WT mice when corrected for body weight (%BW) (Fig. 2b).

To examine the effects of periostin on cystic disease, *Postn*$^{-/-}$ mice were bred with *pcy/pcy* mice to generate *pcy/pcy:Postn*$^{-/-}$ mice. As expected, loss of periostin expression, confirmed by immunoblot analysis (Supplemental Figure S1), caused a reduction in body

weight of *pcy/pcy: Postn*$^{-/-}$ mice from 26.3 ± 0.7 to 22.2 ± 0.7 g (P < 0.01) at 20 weeks of age, similar to the effect in WT mice (Fig. 2a, c). However, in contrast to the lack of an effect of *Postn* knockout on kidney mass in normal mice, *pcy/pcy:Postn*$^{-/-}$ mice showed a dramatic decrease in KW/BW (5.9 ± 0.5 *vs*. 3.9 ± 0.4 %, P < 0.001) compared to *pcy/pcy:Postn*$^{+/+}$ mice (Fig. 2d). To understand the ameliorating effects of periostin loss on kidney enlargement, kidneys from *pcy/pcy:Postn*$^{-/-}$ were sectioned for microscopic examination. Compared to *pcy/pcy:Postn*$^{+/+}$ mice, kidneys from *pcy/pcy:Postn*$^{-/-}$ mice showed a significant reduction in cystic area (Fig. 3a). Measurements of cyst surface area in three non-overlapping representative kidney sections demonstrated decreased cystic area in the *Postn* knockout mice from 42.5 ± 2.4 to 21.8 ± 4.2%; P < 0.005 (Fig. 3b). There was also a 28% reduction in the number of cysts per section (Fig. 3c). Thus, loss of periostin expression results in a significant reduction in pathologic enlargement of *pcy/pcy* kidneys by reducing cyst number and total cystic area.

Effect of periostin on cell proliferation in pcy/pcy kidneys

Previously, periostin was shown to stimulate ADPKD cell proliferation through binding α$_V$-integrins and activation of ILK (12), suggesting that periostin provides a proliferative signal that contributes to renal cyst expansion. To test this, we measured the number of proliferating cells in 20 week-old kidneys of *pcy/pcy:Postn*$^{-/-}$ mice compared to *pcy/pcy:Postn*$^{+/+}$ mice by immunohistochemistry using antibodies to proliferating cell nuclear antigen (PCNA) and Ki-67, nuclear markers for cell proliferation. There were visibly fewer PCNA-positive cells (brown precipitate, arrows) in *pcy/pcy: Postn*$^{-/-}$ compared to *pcy/pcy: Postn*$^{+/+}$ kidney sections (Fig. 4a, b), as confirmed by manual counting positive cells in these sections (Fig. 4e). In contrast, *Postn* knockout in mice without renal cystic disease did not affect the number of PCNA-positive cells in the kidneys (Fig. 4c–e).

To confirm the PCNA results, we measured the number of Ki-67 positive cells by immunofluorescence, normalizing for total cell number using the nuclear stain DAPI. As with PCNA staining, kidney sections from *pcy/pcy: Postn*$^{-/-}$ mice (N = 3) had significantly fewer Ki-67 positive cells than those from *pcy/pcy: Postn*$^{+/+}$ mice (2.6 ± 0.2 *vs*. 0.6 ± 0.2 per field, P < 0.001, Fig. 4f). Taken together, these data support the hypothesis that periostin expression is an important contributor to the proliferation of cystic epithelial cells and promotes cyst expansion and kidney enlargement in *pcy/pcy* mice.

To examine the mechanism by which periostin contributes to cell proliferation, we examined effects of *Postn* knockout on the mTOR pathway. This signaling pathway has been implicated in cyst epithelial cell proliferation, and there is increased phosphorylation of downstream targets of mTOR pathway, S6K and S6, in cystic kidneys of human ADPKD, ARPKD and PKD animals, including the *pcy/pcy* mice (8, 41–43). The mTOR pathway is also known to be a downstream target of ILK (44), which we have shown to be activated by periostin (12). To determine whether *Postn* knockout affects mTOR signaling in *pcy/pcy* mice, kidney lysates were prepared and amounts of phosphorylated S6 (pS6) were determined by immunoblot analysis (Fig. 5). The level of pS6, normalized to total S6 (pS6/S6), was significantly decreased (0.35 ± 0.02 *vs*. 1.13 ± 0.12, N = 3, P < 0.05), despite an increase in total S6 in *pcy/pcy: Postn*$^{-/-}$ kidneys. There was also a 26% decrease in band

intensity for pS6K (P < 0.05, data not shown) in *pcy/pcy: Postn$^{-/-}$* kidneys. These data suggest that diminished activity of the mTOR pathway contributes to the reduction in cell proliferation and cystic area in kidneys of *pcy/pcy:Postn$^{-/-}$* mice.

Influence of periostin on renal interstitial fibrosis in pcy/pcy mice

Periostin directly interacts with components of the ECM, including collagen and fibronectin, and promotes collagen cross-linking and fibrogenesis (18–20). In addition to modulating biomechanical properties of tissues, periostin enhances pro-fibrotic TGF-β signaling and can induce fibrosis (45, 46). To assess the role of periostin in renal interstitial fibrosis in *pcy/pcy* mice, kidney sections were stained with Masson trichrome. There was intense blue staining of the collagen deposition adjacent to cysts of 20-week old *pcy/pcy* kidneys and this staining was significantly reduced in *pcy/pcy:Postn$^{-/-}$* kidneys (Fig. 6). Under a polarizing light, picrosirius red, which specifically stains collagen types 1 and III, visualizes pathogenic fibrils within the interstitium. We found that % area of collagen fibrils within the renal interstitium was reduced in *pcy/pcy* mice lacking periostin compared to *pcy/pcy:Postn$^{+/+}$* mice; however, this difference did not reach statistical significance (P = 0.06) (Fig. 7). Nevertheless, in conjunction with the results from analysis of trichrome staining (Fig. 6), these results suggest that periostin directly or indirectly contributes to renal fibrosis in this model of PKD.

Effect of periostin on renal function and survival of pcy/pcy mice

Since *Postn* knockout significantly reduced cystic index, fibrosis and kidney enlargement in *pcy/pcy* mice, we determined if the loss of *Postn* expression improved renal function. As expected, 20 week-old *pcy/pcy: Postn$^{+/+}$* mice had elevated blood urea nitrogen (BUN: 48.7 ± 7.2 mg/dl; normal range is 8–33 mg/dl) with four of the six mice with values above 40 mg/dl (Fig. 8). By contrast, *pcy/pcy: Postn$^{-/-}$* mice had a BUN of 31.3 ± 5.7 mg/dl, P < 0.05, demonstrating that gene knockout of *Postn* significantly improved renal function in *pcy/pcy* mice.

To further examine the effect of *Postn* expression on disease severity, we compared the kidney morphology of sex-matched *pcy/pcy: Postn$^{+/+}$*, *pcy/pcy: Postn$^{+/-}$* and *pcy/pcy: Postn$^{-/-}$* littermates at 20 weeks. Loss of one allele (*Postn$^{+/-}$*) caused a small reduction in kidney weight and decreased cystic area from 47% to 34%; whereas, complete loss of *Postn* expression reduced kidney weight (%BW) from 5.9 to 2.7% and decreased cystic area to 9%. Previously, periostin expression in *Postn$^{+/-}$* newborn mice was found to be ~30 to 50% of the normal level (40). These data suggest that there was a gene dosage effect of periostin on PKD progression in *pcy/pcy* mice.

Next, we compared the lifespan of *pcy/pcy: Postn$^{+/+}$*, *pcy/pcy: Postn$^{+/-}$* and *pcy/pcy: Postn$^{-/-}$* mice that were fed a standard diet *ad libitum* and monitored daily until natural death. Periostin expressing *pcy/pcy* mice lived to 38.1 ± 2.0 weeks, slightly longer than the 30–36 week time span previously reported (37). Interestingly, mice heterozygous at the periostin locus (*pcy/pcy: Postn$^{+/-}$*) survived to 44.4 ± 2.4 weeks (Fig. 9b, c). Complete knockout of periostin (*pcy/pcy: Postn$^{-/-}$*) resulted in a significant increase in survival to 51.4 ± 4.2 weeks with all the mice in this group living longer than the mean age of death for

the *pcy/pcy:Postn*^{+/+} mice (38.1 ± 2.0 weeks). Taken together, these studies demonstrate that renal expression of periostin in *pcy/pcy* mice accelerates disease progression by stimulating cyst epithelial cell proliferation and interstitial fibrosis, thereby contributing to a decline in renal function and death.

DISCUSSION

Periostin is a member of the matricellular proteins that also includes thrombospondins, osteopontin, βig-H3, SPARC and connective tissue growth factors. These small molecules are secreted into the ECM, where they modulate matrix accumulation and collagen fibrillogenesis and bind cell surface integrins to regulate a variety of cell functions, including cell adhesion, migration, proliferation and survival (18, 21, 22, 24, 25, 32). In this study, we found that periostin contributes importantly to renal cyst enlargement and disease progression in *pcy/pcy* mice. Global knockout of *Postn* in *pcy/pcy* mice 1) caused a significant reduction in the KW/BW ratio, 2) decreased renal mTOR activity, 3) reduced the number of proliferating cells, cyst number and cystic area, 4) decreased renal interstitial fibrosis, 5) preserved renal function, and 6) significantly extended the lifespan of the mice.

Our data suggest that periostin is an important contributing factor for the progression of PKD by promoting the proliferation of cystic cells *in vivo*. We have previously shown that periostin activates ILK, which promotes human ADPKD cell proliferation (12). Here, we show that *Postn* loss in the *pcy/pcy* mouse model diminished the activity of mTOR, a signaling pathway implicated in the aberrant proliferation of renal epithelial cells and formation of cysts in human ADPKD, ARPKD and animal models of PKD, including the *pcy/pcy* mouse (8, 41–43). Moreover, mTOR is known to be activated downstream of ILK, via AKT-dependent phosphorylation of tuberin (TSC2) (44). These results suggest that a periostin-ILK-AKT-mTOR signaling axis may be an important mechanism underlying periostin-stimulated cyst cell proliferation.

Periostin is one of the most highly over-expressed genes in human ADPKD cells compared to normal human kidney epithelial cells (12). In this study, we show that periostin is also highly overexpressed in human ARPKD and multiple mouse models of renal cystic disease. This finding implies that periostin overexpression may be a general feature of cystic kidney disease. The mechanism responsible for aberrant periostin expression in cystic disease remains unclear; however, its expression may reflect its role in development and repair. Periostin is highly expressed in the nephrogenic zone, an active site of cell proliferation and vascularization during renal development (47); however, it is not normally expressed in adult kidney. It is possible that persistent expression of periostin has a pro-proliferative effect on these immature developing tubule cells, contributing to cyst growth. Indeed, ADPKD cystic epithelial cells have been characterized as being arrested at a stage of incomplete differentiation (48). Periostin has also been shown to be elevated by mechanical stress (20). It is possible that fluid accumulation by active fluid secretion into the cyst lumen increases internal pressure to elicit a stress response in mural epithelial cells, leading to periostin expression.

Periostin also plays an important role in tissue repair, including repair after acute myocardial infarction and cardiac fibrosis (49–52). Since renal cyst expansion results in chronic injury (53), aberrant periostin expression may be involved in a futile repair mechanism (9) that contributes to cell proliferation, cyst expansion and ultimately renal fibrosis.

Matricellular proteins, such as periostin, are being considered as potential therapeutic targets to prevent fibrosis. Currently, the role of periostin in other chronic kidney diseases remains unclear. Periostin expression appeared *de novo* within the distal tubules after 5/6 nephrectomy (54) and, following glomerular injury, increased expression was observed in the glomerular tuft, vascular pole, Bowman's capsule and in discreet areas of interstitial fibrosis (55). Periostin staining of human renal biopsies appeared to correlate negatively with renal function, supporting a role for periostin in glomerulosclerosis (55).

It should be noted that 6 different splice variants of periostin, varying in size from 751 to 836 amino acids (83 to 93 kDa) have been identified (26). These isoforms of periostin are determined by the presence or absence of exons 17–21 due to in-frame alternative splicing. It remains unclear whether the various isoforms have tissue specific expression or unique functions. Since it is possible that the splice variants facilitate diverse effects on the regulation of matrix production, fibrosis, and cell proliferation, understanding the contribution of the various isoforms may be important for designing therapies that target periostin function.

In summary, periostin expression is elevated in the kidneys of *pcy/pcy* mice throughout the progression of cystic disease. Global knockout of *Postn* reduced renal mTOR activity, percentage of proliferating cells, cyst growth, kidney enlargement, interstitial fibrosis and the decline in renal function. Genetic ablation of *Postn* also significantly extended the lifespan of *pcy/pcy* mice. We conclude that aberrant expression of periostin and possibly other matricellular proteins that are expressed during renal development and tissue repair may be important modulators of cystic disease progression.

METHODS

Experimental animals and study design

The *pcy/pcy* mouse phenotype is caused by mutations in *Nphp3*, which is orthologous to human nephronophthisis type 3 (38, 56–58). Renal cysts form as segmental dilations predominantly in collecting ducts and distal tubules *in utero* and extend to all nephron segments in later stages of the disease (37). *pcy/pcy* kidneys enlarge to several times normal size and azotemia begins to develop by 18 weeks in association with interstitial fibrosis and progressive decline in renal function, a disease course that is similar to human ADPKD. Generally, *pcy/pcy* mice survive to 30–36 weeks, making this a useful model for investigating the effects of genetic manipulations on disease progression.

Postn$^{-/-}$ mice were generated by insertion of the β-galactosidase gene into exon 1 of the periostin gene, causing a loss of periostin expression (40). This homologous recombination strategy removed the DNA encoding for the translation start site, all of first exon and the part of the first intron, replacing it with the bacterial β-galactosidase reporter gene. Newborn

and one-week old $Postn^{-/-}$ mice are indistinguishable from wild-type littermates; whereas, adult mice have mild dwarfism and defects in periosteum, cartilage, cardiac valves and periodontal ligament, tissues that normally express periostin throughout adulthood (40).

$Postn$ knockout in normal CD-1 mice caused a modest reduction in body weight, but had no effect of kidney mass as a percent on total body weight (Fig. 2a–b). We bred pcy/pcy mice with $Postn^{+/-}$ mice to generate $pcy/pcy: Postn^{+/-}$ mice and these mice were backcrossed into pcy/pcy mice (CD-1) for 6–10 generations. In the first group, littermates of $pcy/pcy: Postn^{-/-}$ and $pcy/pcy: Postn^{+/+}$ mice were sacrificed at 20 weeks of age, blood was collected for measurement of BUN and then both kidneys were removed causing fatal exsanguinations. The left kidney was homogenized in lysis buffer for protein extraction, and the right kidney was immersed in 4% paraformaldehyde, embedded in paraffin, and sectioned for immunohistochemistry. In the second group of pcy/pcy mice, we determined whether periostin expression affected survival by comparing $pcy/pcy: Postn^{+/+}$, $pcy/pcy: Postn^{+/-}$ and $pcy/pcy: Postn^{-/-}$ litermates. All animals were provided food and water *ad libitum* and monitored daily. The protocol for use of these mice was approved by the Institutional Animal Care and Use Committee at the University of Kansas Medical Center.

Periostin PCR genotyping

Genotyping for $Postn$ was determined by PCR analysis of genomic DNA with forward (5′-AGTGTGCAGATGTTTGCTTG-3′) and reverse (5′-ACGAAATACAGTTTGGTAATCC-3′) primers to detect the wild-type allele (~300 bp) and with forward (5′-GCATCGAGCTGGGTAATAAGGGTTGGCAAT-3′) and reverse (5′-GACACCAGACCAACTGGTAATGGTAGCGAC-3′) primers to detect the LacZ in the targeted allele (~800 bp) (40).

Quantitative real-time PCR

Total RNA was isolated from human ARPKD cells and mouse kidney tissues, loaded onto the column of an RNAeasy Mini Kit and eluted with RNase free water (12). RNA quality was verified and cDNA was synthesized using Invitrogen SuperScript III first-strand synthesis system. Relative expression levels were determined by SYBR green real-time PCR. Periostin and GAPDH primers were obtained from SuperArray (Frederick, MD).

Measurement of renal cystic area

Tissue sections (5 µm) of paraffin-embedded kidneys from 20-week old $pcy/pcy: Postn^{+/+}$ and $pcy/pcy: Postn^{-/-}$ mice were collected 500 µm apart from the largest axial section to avoid redundant measurements of the same cysts. Sections were stained with hematoxylin and eosin and images were collected using a dissecting microscope connected to a digital camera. Total number of cysts and cystic cross-sectional surface area (SA) per kidney section were determined by a blinded observer using a morphometic analysis system.

Measurement of cell proliferation

The number of proliferating cells was determined by staining for PCNA and Ki-67. Briefly, tissue sections were deparaffinized, incubated in 0.3% hydrogen peroxide, rinsed in water and then incubated with an anti-PCNA antibody overnight at 4° C. The antigen was detected

using the Zymed SuperPicTure polymer detection kit (Invitrogen) and PCNA-positive cells were visualized using 3,3′-diaminobenzidine. The slides were counter stained with hematoxylin and three images were captured per section for measurement.

Sections were also incubated in anti-Ki-67 antibody (1:100; Abcam, Cambridge, MA) and a secondary anti-rabbit antibody conjugated to AlexaFluor 488 was used to visualize Ki-67 positive nuclei. Nuclei were stained with DAPI in Prolong Gold Antifade mounting reagent (Invitrogen). The number of Ki-67 positive nuclei and total number of nuclei (700–1000 cells/image at 60× magnification) were determined by immunofluorescence using a Nikon Eclipse Ti microscope controlled by Metamorph software.

Measurement of fibrosis

Collagen fibers in kidney sections were stained with Masson trichrome and picrosirus red, as described previously (59, 60). Fibrosis (% SA) was determined by a renal pathologist without prior knowledge of the identity of the specimens (Supplemental Methods). Collagen fibers are highly birefringent and binding of picrosirius red, which is an elongated dye with anisotropic molecular organization, enhances collagen birefringence. Pathogenic collagen fibers appear as thick brilliant red or yellow bundles against a dark background in polarizing light.

Measurement of Blood Urea Nitrogen

Blood was collected at the time of sacrifice and serum was isolated by centrifugation at 1500 × g for 15 min. BUN was determined using an enzymatic conductivity rate method (Beckman Coulter, Brea, CA).

Western Blot Analysis

Kidney lysates were prepared for measurements of periostin, phosphorylated S6 (pS6), total S6 and phosphorylated S6K (pS6K) by immunoblot analysis (61). Proteins (40 μg protein/ lane) were separated by 10% SDS-polyacrylamide gel electrophoresis, transferred to nitrocellulose membrane and incubated overnight at 4° C in primary antibody. Membranes were then washed and incubated with secondary antibody conjugated to horseradish peroxidase. Specific antibody signals were detected using chemiluminescence and band images were quantified using a Fluor-S MAX Multi Imager System (Bio-Rad).

Statistics

Data are expressed as mean and standard error (SE). Statistical significance was determined by unpaired t-test for comparison between $Postn^{+/+}$ and $Postn^{-/-}$ mice.

Supplementary Material

Refer to Web version on PubMed Central for supplementary material.

Acknowledgments

References

1. Grantham JJ. 1992 Homer Smith Award. Fluid secretion, cellular proliferation, and the pathogenesis of renal epithelial cysts. J Am Soc Nephrol. 1993; 3:1841–1857. [PubMed: 8338915]

2. Wilson PD, Hreniuk D, Gabow PA. Abnormal extracellular matrix and excessive growth of human adult polycystic kidney disease epithelia. J Cell Physiol. 1992 Feb.150:360–369. [PubMed: 1734038]

3. Mochizuki T, Wu G, Hayashi T, et al. PKD2, a gene for polycystic kidney disease that encodes an integral membrane protein. Science. 1996; 272:1339–1342. [PubMed: 8650545]

4. Harris PC. Molecular basis of polycystic kidney disease: PKD1, PKD2 and PKHD1. Curr Opin Nephrol Hypertens. 2002 May.11:309–314. [PubMed: 11981261]

5. Rossetti S, Strmecki L, Gamble V, et al. Mutation analysis of the entire PKD1 gene: genetic and diagnostic implications. Am J Hum Genet. 2001 Jan.68:46–63. [PubMed: 11115377]

6. Watnick T, Germino GG. Molecular basis of autosomal dominant polycystic kidney disease. Semin Nephrol. 1999 Jul.19:327–343. [PubMed: 10435671]

7. Qin S, Taglienti M, Nauli SM, et al. Failure to ubiquitinate c-Met leads to hyperactivation of mTOR signaling in a mouse model of autosomal dominant polycystic kidney disease. J Clin Invest. 2010 Oct.120:3617–3628. [PubMed: 20852388]

8. Torres VE, Boletta A, Chapman A, et al. Prospects for mTOR inhibitor use in patients with polycystic kidney disease and hamartomatous diseases. Clin J Am Soc Nephrol. 2010 Jul.5:1312–1329. [PubMed: 20498248]

9. Weimbs T. Regulation of mTOR by polycystin-1: is polycystic kidney disease a case of futile repair? Cell Cycle. 2006 Nov 1.5:2425–2429. [PubMed: 17102641]

10. Wahl PR, Serra AL, Le Hir M, et al. Inhibition of mTOR with sirolimus slows disease progression in Han:SPRD rats with autosomal dominant polycystic kidney disease (ADPKD). Nephrol Dial Transplant. 2006 Mar.21:598–604. [PubMed: 16221708]

11. Wallace DP. Cyclic AMP-mediated cyst expansion. Biochim Biophys Acta. 2011 Oct.1812:1291–1300. [PubMed: 21118718]

12. Wallace DP, Quante MT, Reif GA, et al. Periostin induces proliferation of human autosomal dominant polycystic kidney cells through alphaV-integrin receptor. Am J Physiol Renal Physiol. 2008 Nov.295:F1463–1471. [PubMed: 18753297]

13. Yamaguchi T, Hempson SJ, Reif GA, et al. Calcium restores a normal proliferation phenotype in human polycystic kidney disease epithelial cells. J Am Soc Nephrol. 2006 Jan.17:178–187. [PubMed: 16319189]

14. Yamaguchi T, Nagao S, Wallace DP, et al. Cyclic AMP activates B-Raf and ERK in cyst epithelial cells from autosomal-dominant polycystic kidneys. Kidney Int. 2003 Jun.63:1983–1994. [PubMed: 12753285]

15. Yamaguchi T, Wallace DP, Magenheimer BS, et al. Calcium restriction allows cAMP activation of the B-Raf/ERK pathway, switching cells to a cAMP-dependent growth-stimulated phenotype. J Biol Chem. 2004 Sep 24.279:40419–40430. [PubMed: 15263001]

16. Belibi F, Ravichandran K, Zafar I, et al. mTORC1/2 and rapamycin in female Han:SPRD rats with polycystic kidney disease. Am J Physiol Renal Physiol. 2011 Jan.300:F236–244. [PubMed: 20943770]

17. Song X, Di Giovanni V, He N, et al. Systems biology of autosomal dominant polycystic kidney disease (ADPKD): computational identification of gene expression pathways and integrated regulatory networks. Hum Mol Genet. 2009 Jul 1.18:2328–2343. [PubMed: 19346236]

18. Kudo A. Periostin in fibrillogenesis for tissue regeneration: periostin actions inside and outside the cell. Cell Mol Life Sci. 2011 Oct.68:3201–3207. [PubMed: 21833583]

19. Takayama G, Arima K, Kanaji T, et al. Periostin: a novel component of subepithelial fibrosis of bronchial asthma downstream of IL-4 and IL-13 signals. J Allergy Clin Immunol. 2006 Jul. 118:98–104. [PubMed: 16815144]

20. Norris RA, Damon B, Mironov V, et al. Periostin regulates collagen fibrillogenesis and the biomechanical properties of connective tissues. J Cell Biochem. 2007 Jun 1.101:695–711. [PubMed: 17226767]

21. Bao S, Ouyang G, Bai X, et al. Periostin potently promotes metastatic growth of colon cancer by augmenting cell survival via the Akt/PKB pathway. Cancer Cell. 2004 Apr.5:329–339. [PubMed: 15093540]

22. Gillan L, Matei D, Fishman DA, et al. Periostin secreted by epithelial ovarian carcinoma is a ligand for alpha(V)beta(3) and alpha(V)beta(5) integrins and promotes cell motility. Cancer Res. 2002 Sep 15.62:5358–5364. [PubMed: 12235007]

23. Lindner V, Wang Q, Conley BA, et al. Vascular injury induces expression of periostin: implications for vascular cell differentiation and migration. Arterioscler Thromb Vasc Biol. 2005 Jan.25:77–83. [PubMed: 15514205]

24. Li G, Jin R, Norris RA, et al. Periostin mediates vascular smooth muscle cell migration through the integrins alphavbeta3 and alphavbeta5 and focal adhesion kinase (FAK) pathway. Atherosclerosis. 2010 Feb.208:358–365. [PubMed: 19695571]

25. Shao R, Bao S, Bai X, et al. Acquired expression of periostin by human breast cancers promotes tumor angiogenesis through up-regulation of vascular endothelial growth factor receptor 2 expression. Mol Cell Biol. 2004 May.24:3992–4003. [PubMed: 15082792]

26. Morra L, Rechsteiner M, Casagrande S, et al. Relevance of periostin splice variants in renal cell carcinoma. Am J Pathol. 2011 Sep.179:1513–1521. [PubMed: 21763681]

27. Sorocos K, Kostoulias X, Cullen-McEwen L, et al. Expression patterns and roles of periostin during kidney and ureter development. J Urol. 2011 Oct.186:1537–1544. [PubMed: 21855915]

28. Tai IT, Dai M, Chen LB. Periostin induction in tumor cell line explants and inhibition of in vitro cell growth by anti-periostin antibodies. Carcinogenesis. 2005 May.26:908–915. [PubMed: 15731169]

29. Kruzynska-Frejtag A, Machnicki M, Rogers R, et al. Periostin (an osteoblast-specific factor) is expressed within the embryonic mouse heart during valve formation. Mech Dev. 2001 May. 103:183–188. [PubMed: 11335131]

30. Stanton LW, Garrard LJ, Damm D, et al. Altered patterns of gene expression in response to myocardial infarction. Circ Res. 2000 May 12.86:939–945. [PubMed: 10807865]

31. Norris RA, Kern CB, Wessels A, et al. Identification and detection of the periostin gene in cardiac development. Anat Rec A Discov Mol Cell Evol Biol. 2004 Dec.281:1227–1233. [PubMed: 15532025]

32. Baril P, Gangeswaran R, Mahon PC, et al. Periostin promotes invasiveness and resistance of pancreatic cancer cells to hypoxia-induced cell death: role of the beta4 integrin and the PI3k pathway. Oncogene. 2007 Mar 29.26:2082–2094. [PubMed: 17043657]

33. Riener MO, Fritzsche FR, Soll C, et al. Expression of the extracellular matrix protein periostin in liver tumours and bile duct carcinomas. Histopathology. 2010 Apr.56:600–606. [PubMed: 20459570]

34. Sasaki H, Lo KM, Chen LB, et al. Expression of Periostin, homologous with an insect cell adhesion molecule, as a prognostic marker in non-small cell lung cancers. Jpn J Cancer Res. 2001 Aug.92:869–873. [PubMed: 11509119]

35. Tischler V, Fritzsche FR, Wild PJ, et al. Periostin is up-regulated in high grade and high stage prostate cancer. BMC Cancer. 2010; 10:273. [PubMed: 20534149]

36. Kudo Y, Ogawa I, Kitajima S, et al. Periostin promotes invasion and anchorage-independent growth in the metastatic process of head and neck cancer. Cancer Res. 2006 Jul 15.66:6928–6935. [PubMed: 16849536]

37. Takahashi H, Calvet JP, Dittemore-Hoover D, et al. A hereditary model of slowly progressive polycystic kidney disease in the mouse. J Am Soc Nephrol. 1991 Jan.1:980–989. [PubMed: 1883968]

38. Olbrich H, Fliegauf M, Hoefele J, et al. Mutations in a novel gene, NPHP3, cause adolescent nephronophthisis, tapeto-retinal degeneration and hepatic fibrosis. Nat Genet. 2003 Aug.34:455–459. [PubMed: 12872122]

39. Wallace DP, Hou YP, Huang ZL, et al. Tracking kidney volume in mice with polycystic kidney disease by magnetic resonance imaging. Kidney Int. 2008 Mar.73:778–781. [PubMed: 18185504]

40. Rios H, Koushik SV, Wang H, et al. periostin null mice exhibit dwarfism, incisor enamel defects, and an early-onset periodontal disease-like phenotype. Mol Cell Biol. 2005 Dec.25:11131–11144. [PubMed: 16314533]

41. Gattone VH 2nd, Sinders RM, Hornberger TA, et al. Late progression of renal pathology and cyst enlargement is reduced by rapamycin in a mouse model of nephronophthisis. Kidney Int. 2009 Jul. 76:178–182. [PubMed: 19421190]

42. Shillingford JM, Murcia NS, Larson CH, et al. The mTOR pathway is regulated by polycystin-1, and its inhibition reverses renal cystogenesis in polycystic kidney disease. Proc Natl Acad Sci U S A. 2006 Apr 4.103:5466–5471. [PubMed: 16567633]

43. Bonnet CS, Aldred M, von Ruhland C, et al. Defects in cell polarity underlie TSC and ADPKD-associated cystogenesis. Hum Mol Genet. 2009 Jun 15.18:2166–2176. [PubMed: 19321600]

44. Manning BD, Tee AR, Logsdon MN, et al. Identification of the tuberous sclerosis complex-2 tumor suppressor gene product tuberin as a target of the phosphoinositide 3-kinase/akt pathway. Mol Cell. 2002 Jul.10:151–162. [PubMed: 12150915]

45. Lorts A, Schwanekamp JA, Baudino TA, et al. Deletion of periostin reduces muscular dystrophy and fibrosis in mice by modulating the transforming growth factor-beta pathway. Proc Natl Acad Sci U S A. 2012 Jul 3.109:10978–10983. [PubMed: 22711826]

46. Sidhu SS, Yuan S, Innes AL, et al. Roles of epithelial cell-derived periostin in TGF-beta activation, collagen production, and collagen gel elasticity in asthma. Proc Natl Acad Sci U S A. 2010 Aug 10.107:14170–14175. [PubMed: 20660732]

47. Ito T, Suzuki A, Imai E, et al. Tornado extraction: a method to enrich and purify RNA from the nephrogenic zone of the neonatal rat kidney. Kidney Int. 2002 Sep.62:763–769. [PubMed: 12164857]

48. Calvet JP. Molecular genetics of polycystic kidney disease. J Nephrol. 1998; 11:24–34. [PubMed: 9561482]

49. Conway SJ, Molkentin JD. Periostin as a heterofunctional regulator of cardiac development and disease. Curr Genomics. 2008 Dec.9:548–555. [PubMed: 19516962]

50. Horiuchi K, Amizuka N, Takeshita S, et al. Identification and characterization of a novel protein, periostin, with restricted expression to periosteum and periodontal ligament and increased expression by transforming growth factor beta. J Bone Miner Res. 1999 Jul.14:1239–1249. [PubMed: 10404027]

51. Oka T, Xu J, Kaiser RA, et al. Genetic manipulation of periostin expression reveals a role in cardiac hypertrophy and ventricular remodeling. Circ Res. 2007 Aug 3.101:313–321. [PubMed: 17569887]

52. Snider P, Hinton RB, Moreno-Rodriguez RA, et al. Periostin is required for maturation and extracellular matrix stabilization of noncardiomyocyte lineages of the heart. Circ Res. 2008 Apr 11.102:752–760. [PubMed: 18296617]

53. Grantham JJ, Mulamalla S, Swenson-Fields KI. Why kidneys fail in autosomal dominant polycystic kidney disease. Nat Rev Nephrol. 2011 Oct.7:556–566. [PubMed: 21862990]

54. Satirapoj B, Wang Y, Chamberlin MP, et al. Periostin: novel tissue and urinary biomarker of progressive renal injury induces a coordinated mesenchymal phenotype in tubular cells. Nephrol Dial Transplant. 2012 Jul.27:2702–2711. [PubMed: 22167593]

55. Sen K, Lindenmeyer MT, Gaspert A, et al. Periostin is induced in glomerular injury and expressed de novo in interstitial renal fibrosis. Am J Pathol. 2011 Oct.179:1756–1767. [PubMed: 21854746]

56. Okada H, Ban S, Nagao S, et al. Progressive renal fibrosis in murine polycystic kidney disease: an immunohistochemical observation. Kidney Int. 2000 Aug.58:587–597. [PubMed: 10916082]

57. Gattone VH 2nd, Chen NX, Sinders RM, et al. Calcimimetic inhibits late-stage cyst growth in ADPKD. J Am Soc Nephrol. 2009 Jul.20:1527–1532. [PubMed: 19423689]

58. Omori S, Hida M, Fujita H, et al. Extracellular signal-regulated kinase inhibition slows disease progression in mice with polycystic kidney disease. J Am Soc Nephrol. 2006 Jun.17:1604–1614. [PubMed: 16641154]

59. Montes GS, Junqueira LC. The use of the Picrosirius-polarization method for the study of the biopathology of collagen. Mem Inst Oswaldo Cruz. 1991; 86(Suppl 3):1–11. [PubMed: 1726969]

60. Zhang H, Sun L, Wang W, et al. Quantitative analysis of fibrosis formation on the microcapsule surface with the use of picro-sirius red staining, polarized light microscopy, and digital image analysis. J Biomed Mater Res A. 2006 Jan.76:120–125. [PubMed: 16121387]

61. Nagao S, Nishii K, Yoshihara D, et al. Calcium channel inhibition accelerates polycystic kidney disease progression in the Cy/+ rat. Kidney Int. 2008 Feb.73:269–277. [PubMed: 17943077]

62. Farris AB, Adams CD, Brousaides N, et al. Morphometric and visual evaluation of fibrosis in renal biopsies. J Am Soc Nephrol. 2011 Jan.22:176–186. [PubMed: 21115619]
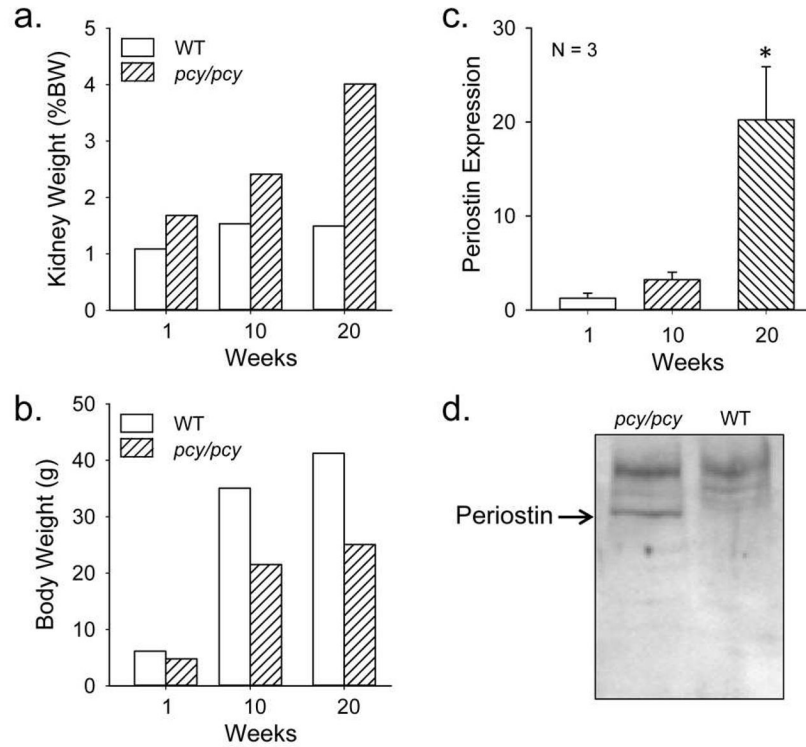
Figure 1. Kidney and body weight, and periostin expression in *pcy/pcy* and wildtype mice

Male *pcy/pcy* mice and wildtype (WT) mice (2–3 mice per group) were sacrificed at 1, 10 and 20 weeks for determination of (**a**) total kidney weight, represented as a percentage of body weight (%BW) and (**b**) body weight. (**c**) Renal periostin (*Postn*) mRNA expression between *pcy/pcy* and WT mice was determined by quantitative real-time RT-PCR. Periostin expression was normalized to GAPDH and the expression in *pcy/pcy* kidneys was represented as fold-change compared to WT kidneys, calculated from C_t (N = 3 per group). Data represent mean ± SE. Statistical analysis was determined by ANOVA and SNK post test. *P < 0.05. (**d**) Immunoblot for periostin protein (90 kDa) in kidneys of 20-week old *pcy/pcy* and WT mice. Expression of periostin protein was confirmed in two additional pairs of *pcy/pcy* and WT mice (Supplemental Figure S1).
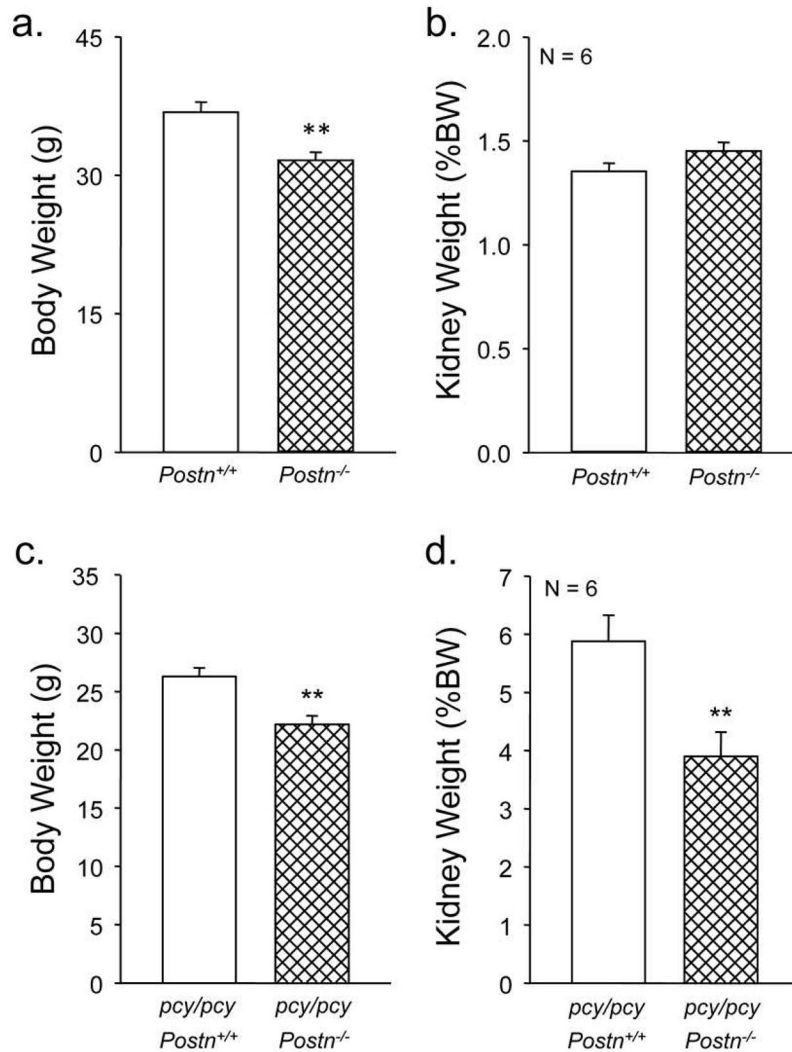
Figure 2. Effect of periostin expression on kidney weight in *pcy/pcy* mice

At 20 weeks, body weights of male *pcy/pcy: Postn*$^{+/+}$ and *pcy/pcy: Postn*$^{-/-}$ mice were measured and kidneys were collected to determine total kidney weight, represented as %BW. **(a)** *Postn*$^{-/-}$ *(CD-1)* mice had a lower body weight than periostin-expressing littermates consistent with mild dwarfism in mice lacking periostin expression (40). **P < 0.001, compared to *Postn*$^{+/+}$ mice. (**b**) By contrast, kidney weight (%BW) was not different between *Postn*$^{-/-}$ and *Postn*$^{+/+}$ mice. **(c)** As expected, *pcy/pcy: Postn*$^{-/-}$ mice also had a lower body weight compared to *pcy/pcy: Postn*$^{+/+}$ mice. **(d)** There was a 34% reduction in kidney weight (%BW) of *pcy/pcy: Postn*$^{-/-}$ mice compared to *pcy/pcy:Postn*$^{+/+}$ littermates. Data are means ± SE. Statistical analysis was determined by an unpaired t-test. **P < 0.001, compared to *pcy/pcy: Postn*$^{+/+}$.
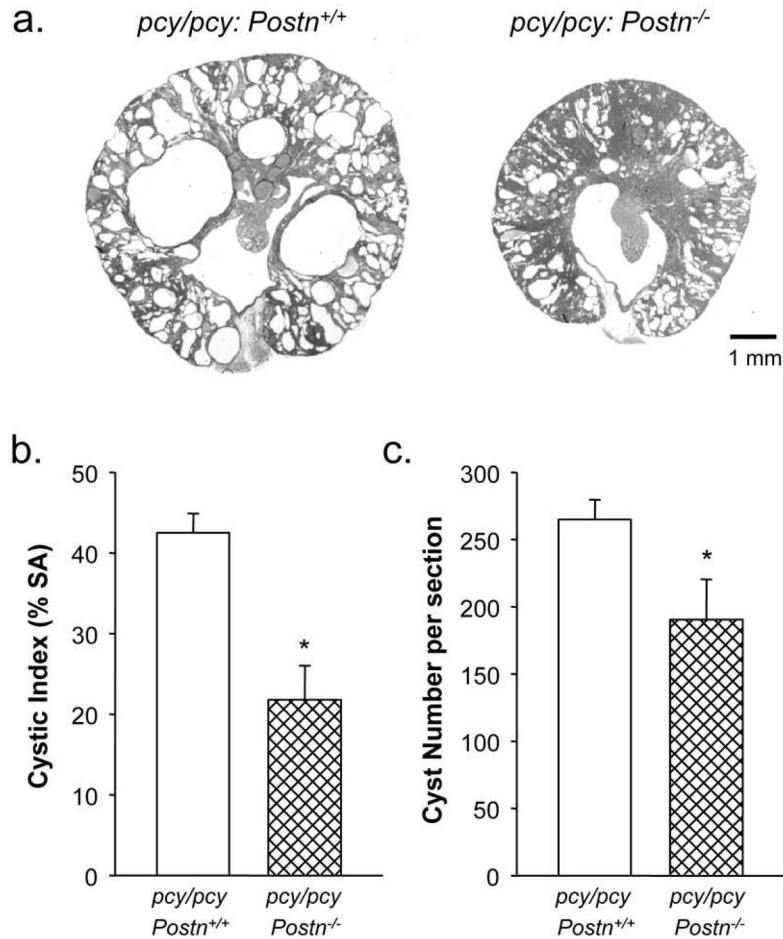
Figure 3. Effect of periostin expression on renal cyst development in *pcy/pcy* mice
(a) Representative kidney sections of male *pcy/pcy: Postn*^{+/+} and *pcy/pcy: Postn*^{−/−} mice.
Scale bar is 1 mm. **(b)** Cross-sectional surface area of cysts is represented as % of total area minus the area of the renal pelvis. Data are mean ± SE from three representative sections per kidney. *pcy/pcy: Postn*^{−/−} kidneys had a marked reduction in cystic area compared to *pcy/pcy: Postn*^{+/+} kidneys. **(c)** The number of cysts (50 μm) per section was also significantly reduced in the *pcy/pcy: Postn*^{−/−} kidneys (190 ± 30 *vs*. 265 ± 15). Data are means ± SE. Statistical analysis was determined by an unpaired t-test. *P < 0.05, compared to the *pcy/pcy: Postn*^{+/+} kidneys.
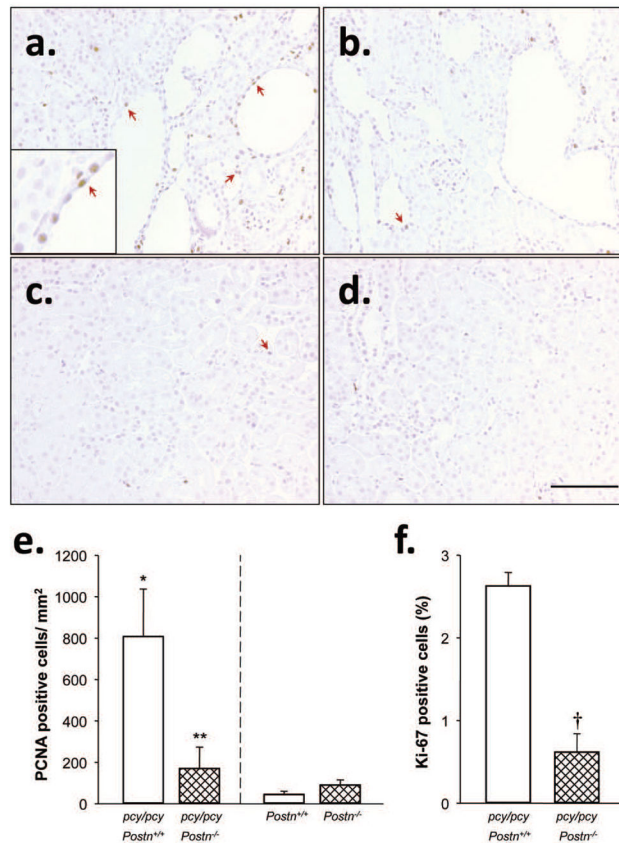
Figure 4. Effect of periostin on cell proliferation in *pcy/pcy* mice

Representative kidney sections from **(a)** *pcy/pcy: Postn*$^{+/+}$, **(b)** *pcy/pcy: Postn*$^{-/-}$, **(c)** *Postn*$^{+/+}$ *(CD-1)*, and **(d)** *Postn*$^{-/-}$ *(CD-1)* mice were stained with an antibody to proliferating cell nuclear antigen (PCNA), a proliferation marker. All images were taken at the same magnification. Bar scale is 100 μm. The inset in the lower left corner of Fig. 4a shows a higher magnification image of brown-stained nuclei of PCNA-positive cells. Sections were counter stained with hematoxylin. **(e)** The number of PCNA-positive cells per section area (excluding cyst lumens) from three random microscope images was determined by an observer blinded to the identity of the slides. There were significantly fewer PCNA-positive cells in *pcy/pcy* mice lacking periostin, compared to *pcy/pcy:Postn*$^{+/+}$ kidneys. **(f)** To further examine the effect of *Postn* deletion on cell proliferation, three tissue sections/ kidney (N = 3 kidneys) were stained with an antibody to Ki-67, another proliferation marker. Ki-67 was visualized using a secondary antibody conjugated to GFP and the number of Ki-67 positive cells was quantified by counting GFP-positive cells using a Nikon immunofluorescence microscope controlled by Metamorph software. Total cell numbers were determined by counting nuclei stained with DAPI and data are presented as % of Ki-67 positive cells. There were fewer Ki-67 positive cells in *pcy/pcy: Postn*$^{-/-}$ kidney sections compared to the *pcy/pcy: Postn*$^{+/+}$ kidney sections, confirming the PCNA results. Data are means ± SE. Statistical analysis was determined by unpaired t-test. *P < 0.05, compared to *Postn*$^{+/+}$ *(CD-1)*; **P < 0.05 and †P < 0.001, compared to *pcy/pcy: Postn*$^{+/+}$.
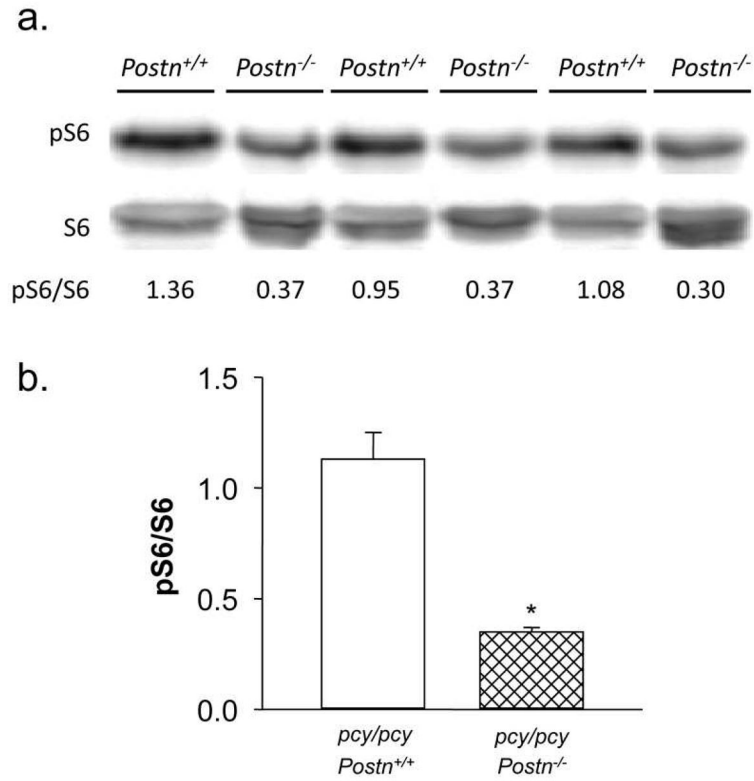
Figure 5. Effect of periostin expression on mTOR signaling in *pcy/pcy* mice
(a) Immunoblot analysis was used to compare the effect of *Postn* deletion on
phosphorylation levels of the ribosomal protein S6 (pS6), a downstream target of the mTOR
signaling pathway, in kidneys of *pcy/pcy* mice. Levels of pS6 were normalized to total S6.
The number below the bands indicates the pS6/S6 for each sample. **(b)** Summary of the
effect of *Postn* knockout in *pcy/pcy* mice on renal pS6/S6 levels. Data are means ± SE.
Statistical analysis was determined by unpaired t-test. *P < 0.05, compared to *pcy/pcy:
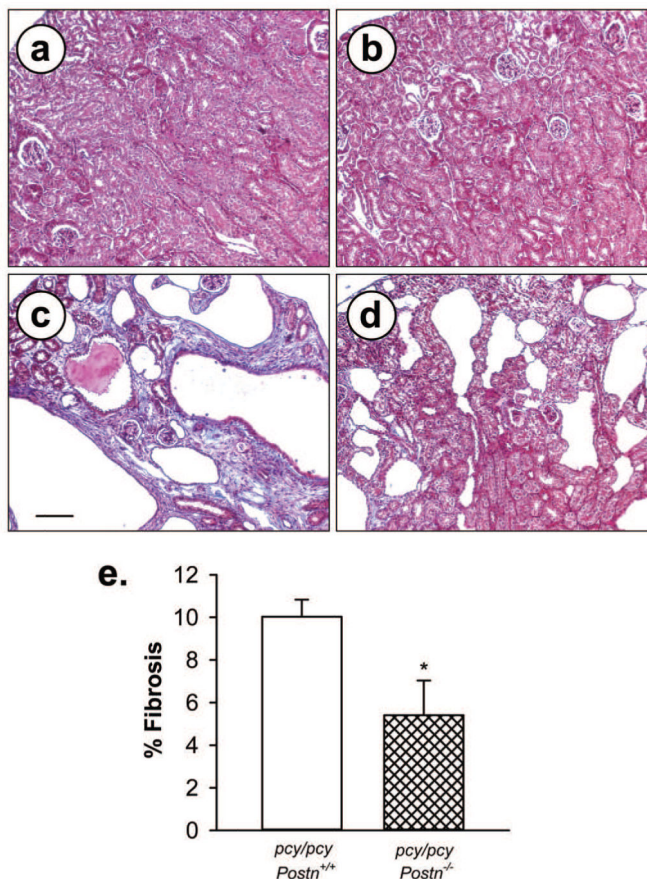Postn*^{+/+} kidney, N = 3.

Figure 6. Effect of periostin expression on interstitial collagen deposition in *pcy/pcy* mice
Representative kidney sections from (**a**) $Postn^{+/+}$, (**b**) $Postn^{-/-}$, (**c**) *pcy/pcy: Postn*$^{+/+}$ and (**d**) *pcy/pcy: Postn*$^{-/-}$ mice were stained with Masson trichrome to visualize collagen deposition. There was intense staining of collagen (blue color) within the interstitial areas adjacent cysts in *pcy/pcy* mice expressing *Postn*. By contrast, collagen staining was markedly reduced in cystic areas of *pcy/pcy: Postn*$^{-/-}$ mice. All images are the same magnification. Bar scale is 100 μm. (e) Fibrosis was determined by visual assessment of the trichrome-stained slides and represented as % fibrotic area to total area of the whole tissue section. Sections (n = 6 per group) were de-identified and fibrosis was determined by visual measurement of % fibrotic area (62). Data are means ± SE. Statistical analysis was determined by unpaired t-test. *P < 0.05, compared to *pcy/pcy: Postn*$^{+/+}$ kidney.
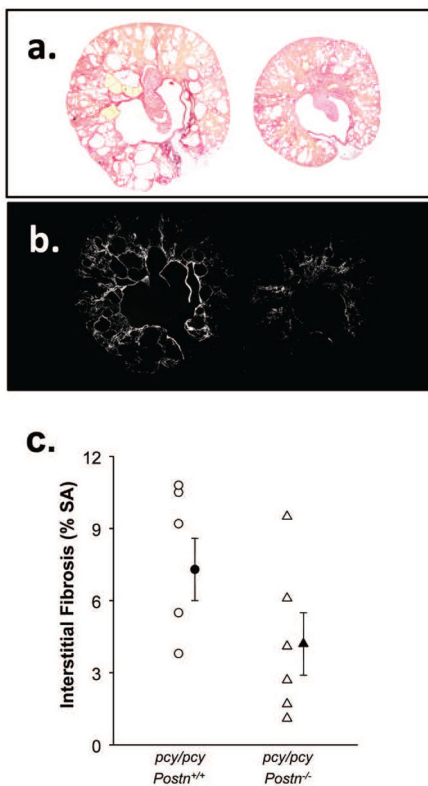
Figure 7. Effect of periostin expression on fibrillar collagen in *pcy/pcy* kidneys
(a) Kidney sections of *pcy/pcy: Postn*$^{+/+}$ (left) and *pcy/pcy: Postn*$^{-/-}$ (right) mice were stained with picrosirius red (59, 60) and illuminated with a polarized light to visualize type I and III collagen fibrils **(b).** Images were digitized with the use of a computer-video analysis system and converted to gray scale for measurement of the area of white pathogenic collagen fibers as a % of total surface area (SA) **(c).** There was a trend for less collagen fibrils in tissue sections of *pcy/pcy: Postn*$^{-/-}$ kidneys compared to *pcy/pcy: Postn*$^{+/+}$ kidneys; however, the difference did not reach statistical significance (P = 0.06) by an unpaired t-test. Data are means ± SE.
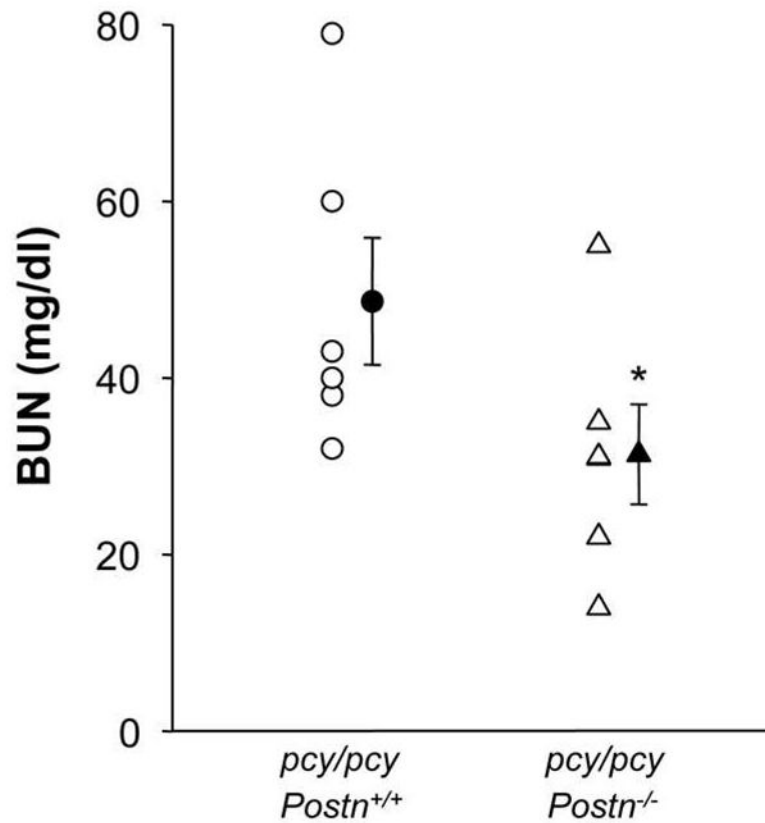
Figure 8. Effect of periostin expression on blood urea nitrogen (BUN) in *pcy/pcy* mice

At 20 weeks, *pcy/pcy: Postn*^{+/+} mice had a BUN of 48.7 ± 7.2 mg/dl with five of the six mice with values above 33 mg/dl. The normal range for BUN in healthy adult mice is 8 to 33 mg/dl. By contrast, the mean BUN for *pcy/pcy: Postn*^{−/−} mice was 31.3 ± 5.7 mg/dl (P < 0.05), consistent with improved renal function. Data are means ± SE. Statistical analysis was determined by unpaired t-test.
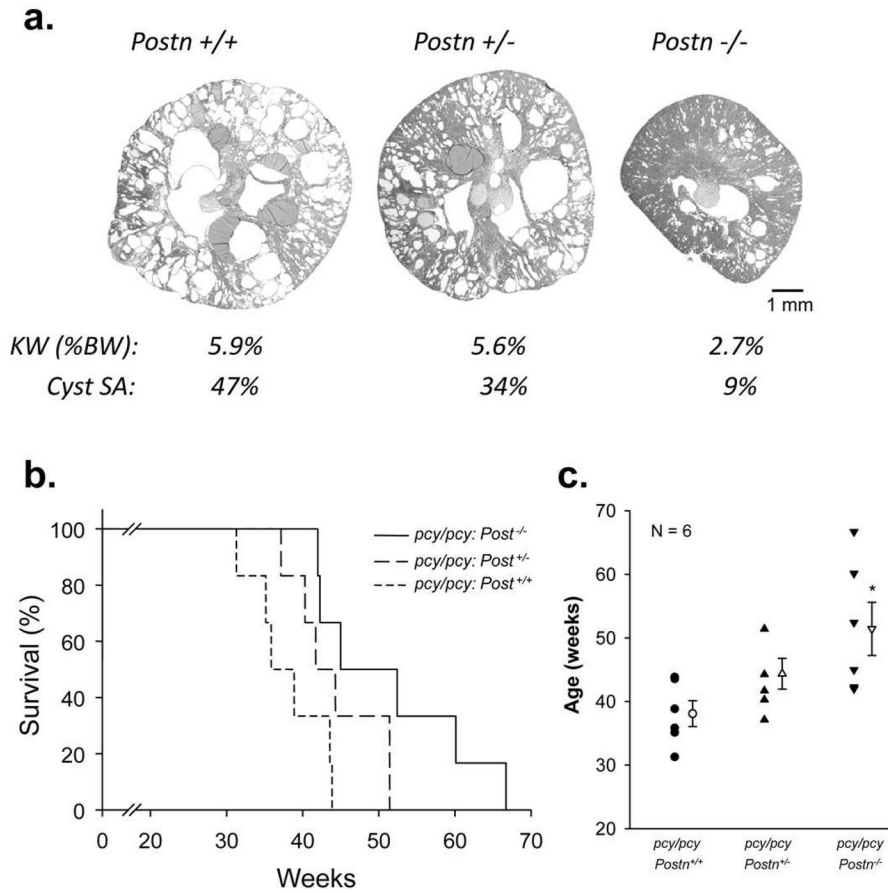
Figure 9. Effect of periostin expression on the lifespan of *pcy/pcy* mice

The lifespan of *pcy/pcy* mice is 30–36 weeks of age and death is typically caused by renal failure (37). To determine whether periostin expression affects the survival of *pcy/pcy* mice, littermates of *pcy/pcy: Postn*^{+/+}, *pcy/pcy: Postn*^{+/−} and *pcy/pcy: Postn*^{−/−} mice were given standard diet *ad libitum* until natural death. (**a**) Representative images of kidney sections, kidney weight (KW) as %BW, and % cystic area from *pcy/pcy: Postn*^{+/+}, *pcy/pcy: Postn*^{+/−} and *pcy/pcy: Postn*^{−/−} mice at 20 weeks of age. (**b**) Kaplan-Meier curve of *pcy/pcy: Postn*^{+/+}, *pcy/pcy: Postn*^{+/−} and *pcy/pcy: Postn*^{−/−} mice. (**c**) Summary of the age of death. *pcy/pcy: Postn*^{+/+} mice died at 38.1 ± 2.0 weeks. By contrast, *pcy/pcy* mice with the loss of one *Postn* allele (*pcy/pcy: Postn*^{+/−}) survived to 44.4 ± 2.4 weeks and *pcy/pcy* mice with a complete loss of periostin expression survived to 51.4 ± 4.2 weeks (*$P < 0.05$, compared to *pcy/pcy: Postn*^{+/+}). Data are means ± SE. Statistical analysis was determined by ANOVA and SNK post test.

Table 1

Periostin mRNA levels in recessive models of PKD

	_N_	**Fold Increase**
Human ARPKD _vs_. NHK cells	3	19.6
cpk/cpk mouse kidney _vs_. WT tissue (3 weeks)	3	9.3
jck/jck mouse kidney _vs_. WT tissue (20–25 weeks)	3	> 50